

# X-ray and optical observations of the Shapley supercluster in Hydra–Centaurus

Somak Raychaudhury<sup>1</sup>, A. C. Fabian<sup>1</sup>, A. C. Edge<sup>1</sup>, C. Jones<sup>2</sup> and W. Forman<sup>2</sup>

<sup>1</sup>*Institute of Astronomy, Madingley Road, Cambridge CB3 0HA*

<sup>2</sup>*Harvard–Smithsonian Center for Astrophysics, 60 Garden Street, Cambridge MA 02138, USA*

Accepted 1990 August 13. Received 1990 August 8; in original form 1990 April 17

## SUMMARY

X-ray and optical observations of the ‘Shapley Supercluster’, at redshifts between 0.037 and 0.053 in the region of Hydra and Centaurus, are presented. The X-ray data show that many of the clusters are multiple and confirm the exceptionally high density of rich clusters. Six of the 46 X-ray brightest clusters at high galactic latitude belong to this supercluster. The Local Supercluster is less luminous in X-rays than the least-luminous cluster found here, and only the Centaurus cluster in the Hydra–Centaurus Supercluster (the Great Attractor) is (just) more luminous than the weakest cluster detected in the Shapley Supercluster. The optical and X-ray luminosity functions suggest that there are large deviations from the Hubble flow in the region and that clusters are merging at a high rate. The minimum mass of the supercluster, obtained by summing the masses of the separate clusters estimated from their X-ray luminosity, exceeds  $1.4 \times 10^{16} h_{50}^{-1} M_{\odot}$ . This is consistent with the mass estimated from optical-dipole measurements. The ratio of mass density in observed clusters to the mean density of the Universe exceeds  $0.8 \Omega_0^{-1}$  over the core region of radius  $37 h_{50}^{-1}$  Mpc.

## 1 INTRODUCTION

Sixty years ago, Shapley (1930) noted a ‘remote cloud of galaxies’ in Centaurus and Hydra which is rich in clusters of galaxies. He found it particularly interesting because of its ‘great linear dimension, the numerous population and distinctly elongated form’ and noted that it has an ‘indefinite extension’ to the north into the Corvus–Virgo region. This cloud, which we call here the ‘Shapley Supercluster’, has recently been noted from galaxy-velocity measurements (Melnick & Moles 1987) and the distribution of optical galaxies (Raychaudhury 1989) and *IRAS* galaxies (Allen *et al.* 1990), and from all-sky samples of Abell clusters (Scaramella *et al.* 1989) and X-ray clusters (Lahav *et al.* 1989).

Our optical data consist of magnitudes and positions of 21 000 galaxies in  $0.8 \text{ sr}$  of the sky in the direction of Hydra–Centaurus, obtained with the APM facility at Cambridge which was used to search for galaxies on UK Schmidt plates (Raychaudhury 1989, 1990). Redshifts for 34 clusters in this region can be found in the literature. Fig. 1 clearly shows that almost all these clusters belong to two distinct groups. The nearer group is what is commonly known as the ‘Hydra–Centaurus Supercluster’ at a mean redshift of  $3980 \text{ km s}^{-1}$ . This supercluster is currently the best candidate for the putative ‘Great Attractor’ (Lynden-

Bell *et al.* 1988). On the other hand, almost all of the remaining 17 clusters, lying between  $11\,000 < v < 16\,000 \text{ km s}^{-1}$  are within  $10^\circ$  of A3558 (Shapley 8). The mean redshift of these clusters is  $\bar{v} = 13\,700 \text{ km s}^{-1}$ , and it is this concentration that we call here the ‘Shapley Supercluster’.

Since this supercluster lies in a rich region of the Local Supergalactic Plane, further studies are hampered by the effects of projection, which make the identification of the individual cluster components difficult if only optical galaxy counts are used. X-ray observations are much less susceptible to these effects since the X-ray luminosity of a cluster varies roughly as the cube of the number density of galaxies (Edge & Stewart 1990). In Section 2 of this paper, we present X-ray images from the *Einstein Observatory* and *EXOSAT* of seven of the main galaxy concentrations in the supercluster. These are resolved into 12 separate clusters and compared in Section 3 with optical galaxy counts of the same region. This result emphasizes the richness of the region.

Recent work on an X-ray flux-limited sample of clusters (Edge *et al.* 1990) has shown evidence for strong evolution of high-luminosity clusters. This is interpreted as evolution due to merging of clusters and subclusters on time-scales of  $\sim 10^{10}$  yr. In regions of high cluster density the merging time-scale may decrease and the evolution of clusters in these regions may be more rapid than in the ‘field’ population. We

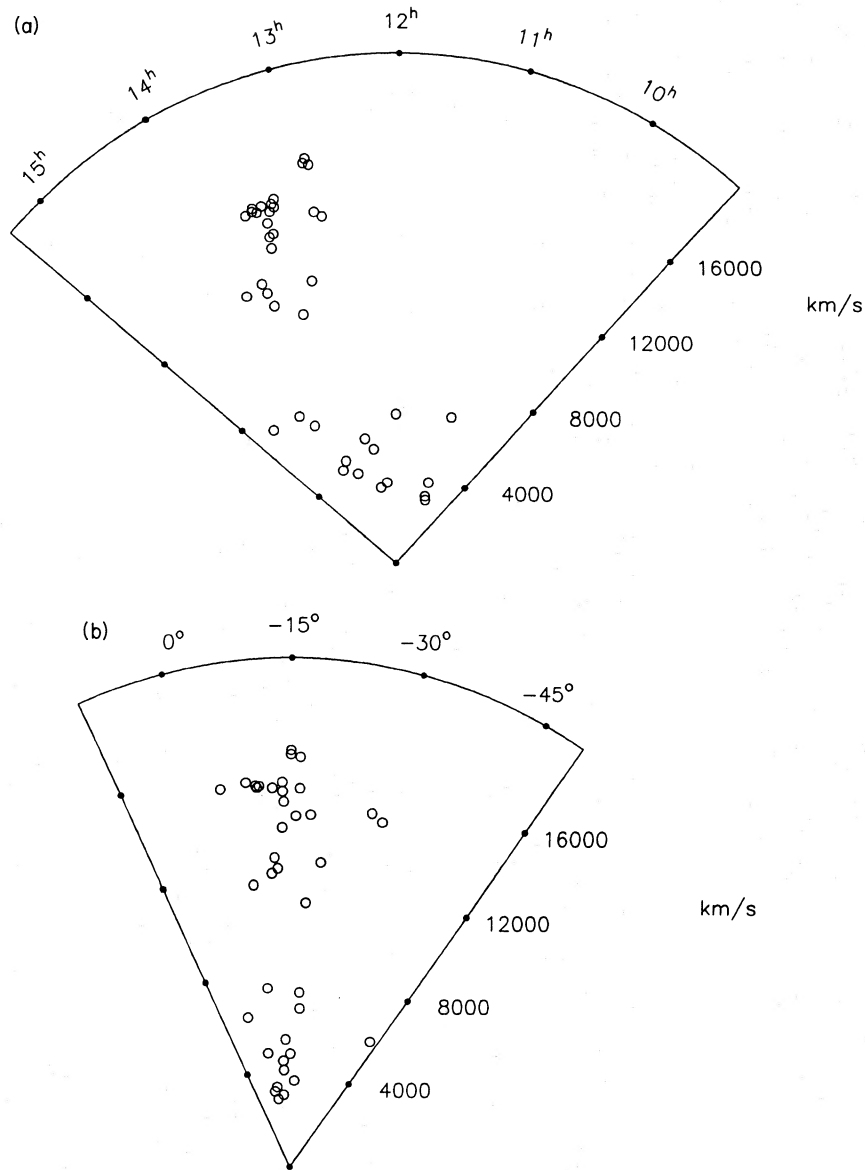


**Figure 1.** Wedge diagrams of galaxy clusters in the direction of Hydra–Centaurus, with known redshifts, showing the position on the sky [(a) Right Ascension, (b) Declination] against mean redshift. The plots clearly show the existence of two distinct groups of clusters. The nearer group, between  $2800\text{--}5000\text{ km s}^{-1}$ , is known as the ‘Hydra–Centaurus Supercluster’. The further group, between  $11\,000 < v < 16\,000\text{ km s}^{-1}$ , is the ‘Shapley Supercluster’, the mean redshift being  $\langle v \rangle = 13\,700\text{ km s}^{-1}$ . Note the absence of clusters between  $5000$  and  $10\,000\text{ km s}^{-1}$ , and beyond  $3500\text{ km s}^{-1}$  in the range  $9^{\text{h}} < \text{RA} < 12^{\text{h}}30^{\text{m}}$ .

interpret the current state of the Shapley Supercluster in terms of such evolution in Section 4 from the X-ray cluster-luminosity function in the supercluster. The optical-luminosity functions of the individual clusters are used to search for deviations from the Hubble flow.

The mass of the Shapley Supercluster is estimated in several ways in Section 5. A minimum mass is obtained by scaling to the mass of the Coma cluster using the X-ray luminosities of the component clusters. The minimum mass-to-light ratio of the supercluster is comparable to that for typical clusters elsewhere. Finally, in Section 6, the overdensity of the core of the supercluster is shown to be large, and some of the consequences of such a massive concentration of clusters are explored.

## 2 X-RAY DATA

We have collected together all the available X-ray images of clusters in the Hydra, Centaurus and Virgo region bounded by  $\text{RA} = 12^{\text{h}}50^{\text{m}}$  to  $14^{\text{h}}$  and  $\text{Dec.} = -13^{\circ}$  to  $-37^{\circ}$  shown in Fig. 2(a). The supercluster can be split into three parts; the core around Shapley 8 (A3558), the western extension composed of A3528 and A3530/A3532, and the northern extension of A1631 and A1644. The velocities of the clusters range from  $11\,000$  to  $16\,000\text{ km s}^{-1}$ .

The region contains six of the 46 X-ray-brightest clusters at  $|b| > 20^{\circ}$  (Edge *et al.* 1990). This means that 13 per cent of the brightest clusters lie in 1.4 per cent of the sky (excluding the unsampled region  $|b| \leq 20^{\circ}$ ). We find in the present work

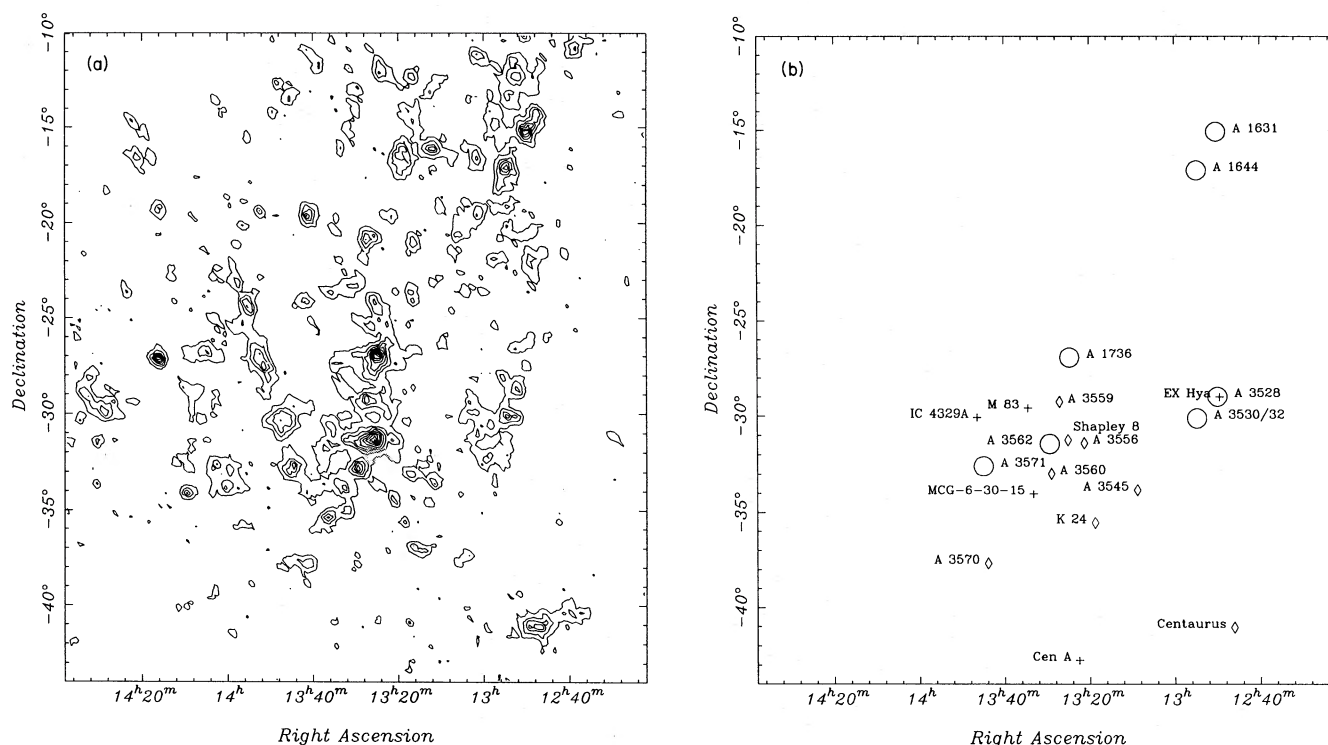


**Figure 2.** (a) An isopleth map of galaxies brighter than  $B_r = 17$  mag in a  $34^\circ \times 34^\circ$  region of the sky around Shapley 8, showing the major features of the Shapley Supercluster. The horizontal spur consisting of four rich clusters of galaxies represents Shapley's (1930) 'remarkable cloud of galaxies' in Centaurus. The galaxies were binned in  $0.25 \text{ deg}^2$  bins, and the isopleths were prepared in the same way as in Fig. 3 (see text). (b) Identification chart drawn on the same scale as (a). Circles of radius  $0.05'$  indicate the IPC and *EXOSAT* fields used in Fig. 3. Positions of a few other important clusters (diamonds) and other X-ray sources (+) are indicated.

yet another (double) cluster in the region, A3528, confused with the cataclysmic variable EX Hya, that should be in the X-ray-brightest list. The concentration is even more remarkable when it is noted that the clusters also occur within a redshift interval of  $\Delta z = 0.015$ . The region also contains (Fig. 2b) bright X-ray sources such as the cataclysmic variable EX Hya, the spiral galaxy M83 and the active galaxies MCG-6-30-15 and IC4329A. The radio galaxy Centaurus A lies outside the region to the south and the Centaurus and Hydra clusters lie to the south-west and west, respectively. The concentration of clusters contributes only a small fraction ( $< 25$  per cent) of the X-ray excess observed by Jahoda & Mushotzky (1989).

The cluster images are presented in Fig. 3. They were made with the Imaging Proportional Counter (IPC) on the *Einstein Observatory*, apart from that of A3571 which was made with *EXOSAT*. The images reveal that several of the clusters have companions and are therefore resolved into two or more clusters. On the basis of clearly resolved X-ray emission, only A1631, A1736 and A3571 appear to be single-peaked images. A1644, A3528 and A3532 (with A3530) are clearly double peaked and the image just east of Shapley 8, containing A3562, has three peaks. A3532 (with A3530) and A3528 form a hierarchical 'double-double' system, reminiscent of multiple-star systems. A1736 is probably not double since its south-east X-ray peak, is unresolved. Its velocity distribution is double-peaked (Dressler & Shectman 1988a), but from Dressler & Shectman's (1988b) data, it seems that their lower-velocity

clump may not represent a bound cluster. The fraction of clusters in this region that are multiple ( $> 50$  per cent) is much higher than in the 'field' ( $\sim 10$  per cent, Forman *et al.* 1981).

The 2–10-keV X-ray luminosities (assuming  $H_0 = 50 \text{ km s}^{-1} \text{ Mpc}^{-1}$ ) of the clusters are given in Table 1. For four of the clusters (A1736, A3532, A3562 and A3571), this is a direct measurement from either the *Einstein Observatory* MPC or the *EXOSAT* ME. There is also a direct measurement of the sum of both components of A1644, and we have a lower limit for A3558 (Shapley 8). We have estimated a 2–10-keV luminosity from each *Einstein Observatory* image by scaling the flux measured within 0.25, 0.5 or 1 Mpc in the IPC (depending upon the proximity of the cluster to the edge of the field) to a total 2–10-keV flux, assuming a King profile and core radius of 500 kpc. The scaling has been normalized to give agreement for the A1644 pair and so is not very sensitive to the assumed core radius. There are considerable uncertainties in the luminosities of some clusters (e.g. A3562 and A3528) due to their observed position in the field.

We have also noted in Table 1 whether the cluster appears to contain a cooling flow about the central galaxy and the mass-deposition rate,  $\dot{M}$ , were well determined by the deprojection technique (Arnaud 1988; Edge 1989). The rates are typical for the X-ray luminosity range (see Pesce *et al.* 1990). We have not yet found a massive flow with  $\dot{M} > 100 M_\odot \text{ yr}^{-1}$  in this supercluster.

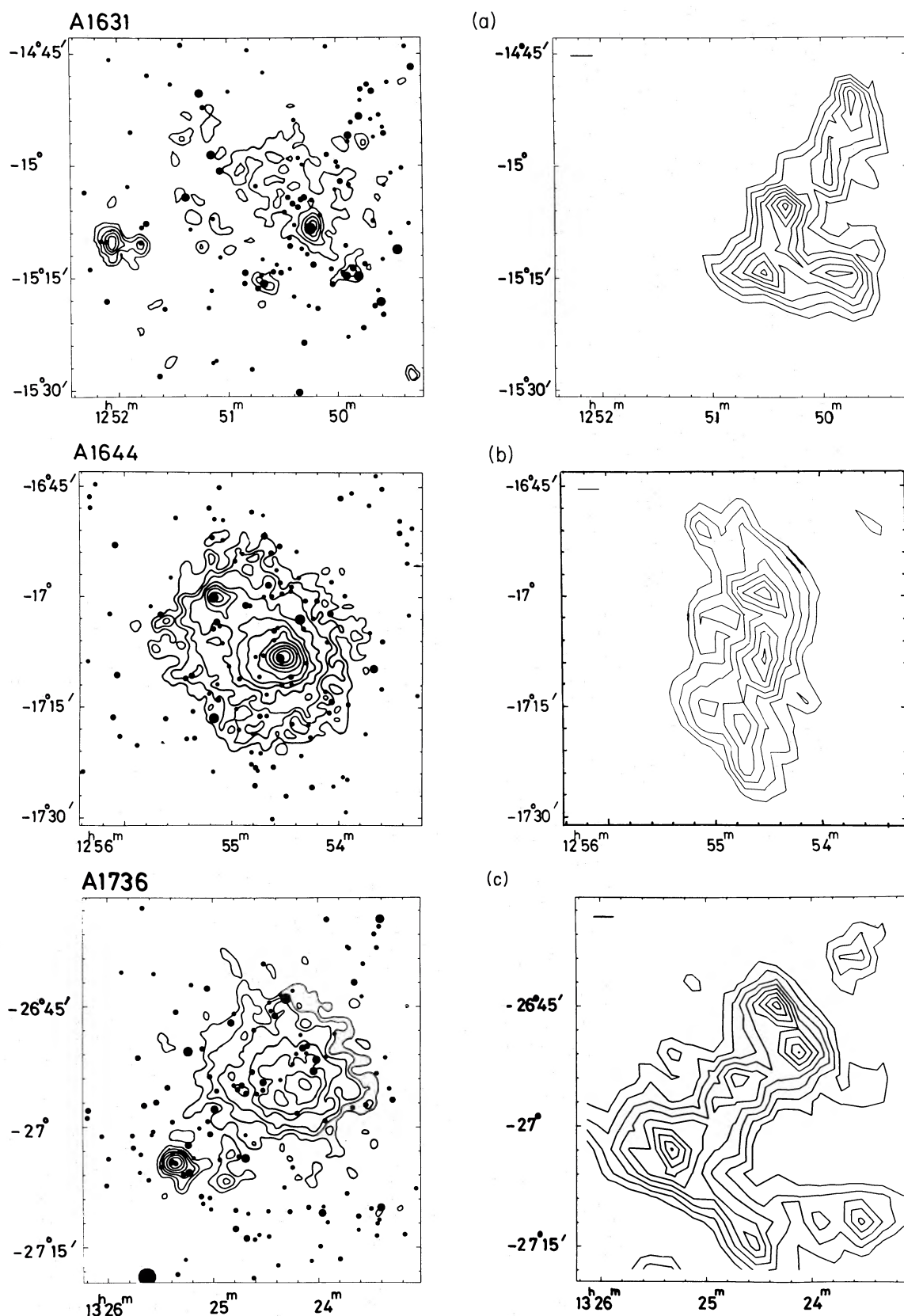


**Figure 3.** (a)–(g) Each panel consists of two plots. Left; a plot of galaxies down to a faint magnitude (typically  $B_r = 18$ ) in a small area of sky (typically  $48 \times 48$  arcmin<sup>2</sup>) around each cluster in Table 1. The galaxies are plotted as filled circles whose areas are proportional to that of the galaxy as measured by the APM. The X-ray map of the same area obtained by the *Einstein* IPC [*EXOSAT* LE in the case of (g)] is superposed on it. In some fields the edge of the IPC field of view or the window-support ribs modify the X-ray map (see Table 1). Right; isopleths of galaxy distribution, in the same area of sky, where only positions of galaxies are used, and all galaxies are weighted equally. The bar on the top left-hand corner shows the size of the bin used. See Table 1 for further description of the separate images.

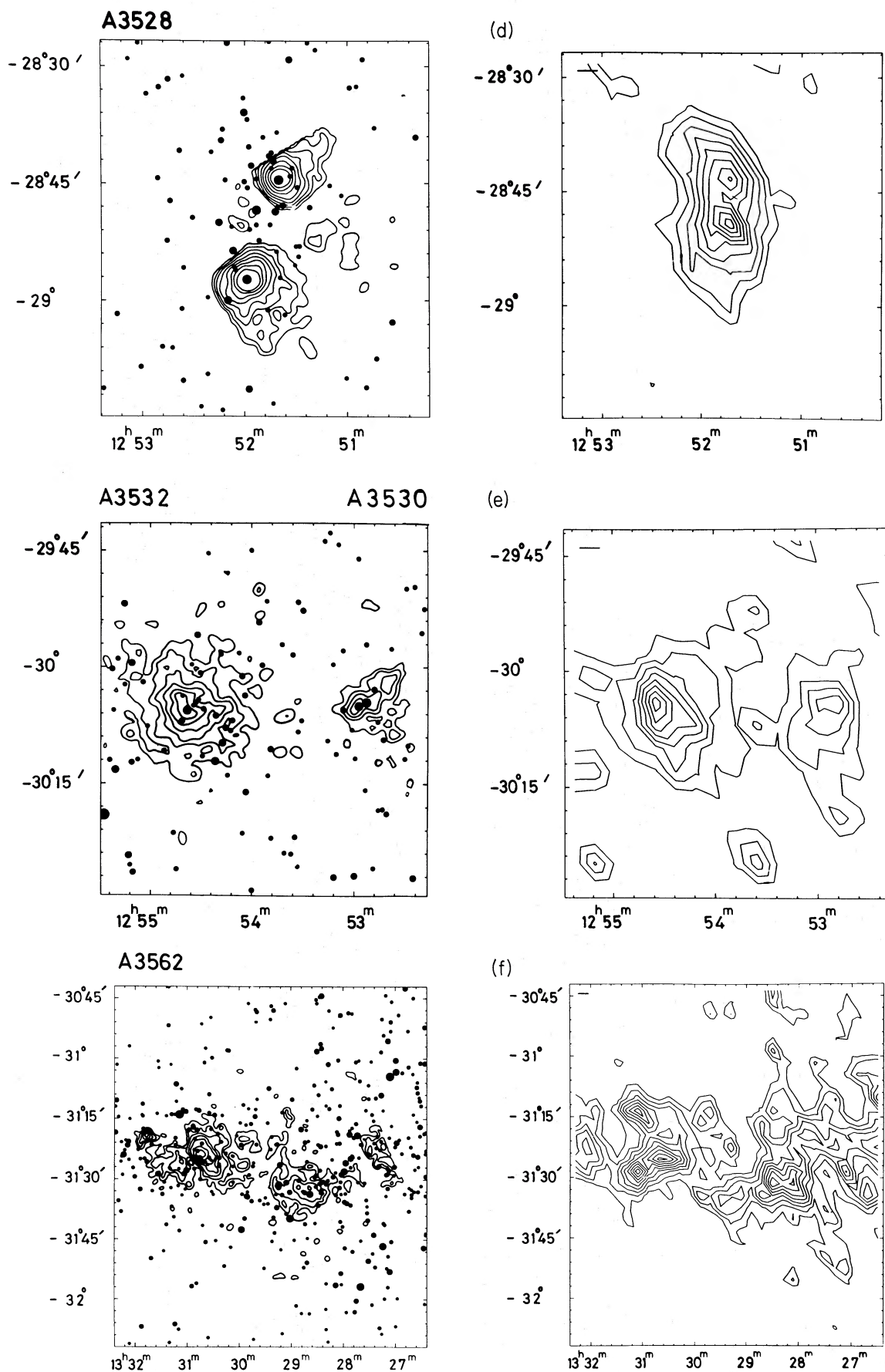


Figure 3 - continued.

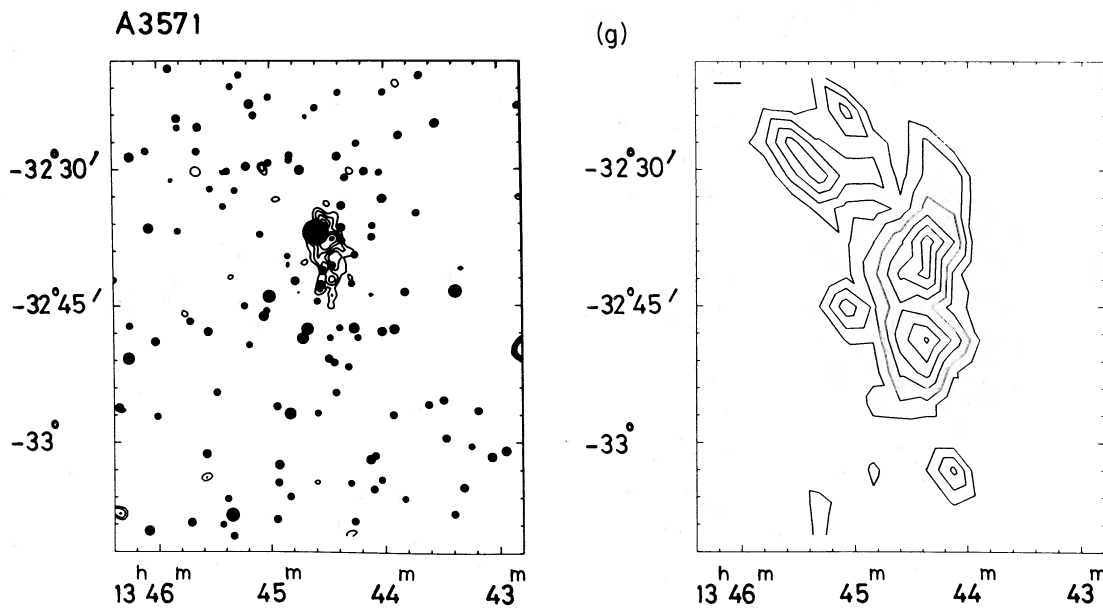


Figure 3 - continued.

### 3 APM DATA

An area of  $2^\circ \times 2^\circ$  around each cluster centre was searched for galaxies down to a limit of  $B_J = 18$  mag on glass copies of UK Schmidt Telescope Unit Sky Survey plates (emulsion IIIa-J). The plates were scanned by the Automatic Plate Measuring (APM) facility in Cambridge. This is a high-speed microdensitometer, which performs on-line image detection and outputs a list of images detected above a certain preset threshold, together with various profile parameters and isophotal magnitudes for each image (details in Kibblewhite *et al.* 1984). The preliminary star-galaxy separation was carried out according to the usual APM galaxy survey procedure (Raychaudhury 1990): this process gives a list of galaxy candidates (typically about 4000 per  $5^\circ \times 5^\circ$  Schmidt plate down to  $B_J = 18$  mag) which is demonstrably about 98 per cent complete. All galaxy candidates in the  $2^\circ \times 2^\circ$  square around each cluster centre were then inspected, and the galaxies were assigned a rough morphological classification.

The APM gives an uncalibrated measure for the sky-subtracted isophotal intensity in each galaxy image above the scan threshold, from which their magnitudes may be obtained. These magnitudes have been reduced to a consistent system by using the galaxies in the overlaps between neighbouring plates (Maddox *et al.* 1990), and calibrating the zero-points using CCD photometry of several galaxies found from different plates. The zero-point data come from the APM survey of galaxies down to a limit of  $B_J = 17$  mag from 110 Schmidt plates in the Hydra-Centaurus direction (Raychaudhury 1990).

The galaxies in and around each cluster were binned such that the mean occupancy of each square bin is half a galaxy, and the bin counts were smoothed using Gaussians of  $\sigma = 1$  bin (truncated at  $3\sigma$ ). The background count was determined by finding the peak of the counts per bin histogram. Isopleth contours were drawn at integral multiples of three times the background count.

In most cases, the isopleths confirm the rich structure shown in the X-ray images. Of some note are A3528 and A1644, where there is no secondary peak in the isopleths coincident with the second X-ray peak, although the X-ray peak coincides with a bright galaxy. This is in part due to the threshold used for the optical counts, which was set so as to be well above background, and to the fact that the isopleths are not luminosity weighted. Furthermore, some of the clusters may be optically poor (some poor clusters are observed to be X-ray bright; Schwartz, Schwarz & Tucker 1980; Kriss, Cioffi & Canizares 1983). The X-ray images show that optical isopleths are not a reliable guide to the true galaxy distribution in crowded regions.

In Fig. 2, there are 17 optical clusters in the Shapley Supercluster (12 of them are ACO rich clusters). Apart from the clusters reported here, which have X-ray observations, there are A3545 ( $v = 11\,550$  km s $^{-1}$ ), K24 ( $v = 14\,970$  km s $^{-1}$ ), A3556 ( $v = 14\,700$  km s $^{-1}$ ), A3559 ( $v = 13\,300$  km s $^{-1}$ ), A3560 ( $v = 14\,850$  km s $^{-1}$ ) and A3570 ( $v = 11\,160$  km s $^{-1}$ ), all within  $10^\circ$  of Shapley 8. The total number of clusters, with present subclusters, is  $\geq 20$ .

### 4 LUMINOSITY FUNCTIONS

We have constructed both the (optical) galaxy-luminosity functions within the individual clusters and the (X-ray) cluster-luminosity function within the supercluster. The former is a diagnostic of the distances of the individual clusters, the latter of the evolution of the supercluster.

The optical-luminosity functions of nine clusters in the supercluster were obtained (Raychaudhury 1990) by binning all the galaxies brighter than  $B_J = 17.5$  mag within a radius of  $2 h_{50}^{-1}$  Mpc of the cluster centre ( $24.5$  arcmin at  $14\,000$  km s $^{-1}$ ;  $H_0 = 50 h_{50}$  km s $^{-1}$  Mpc $^{-1}$ ), in bins  $0.2$ -mag wide, after correcting the magnitudes for galactic extinction using Burstein & Heiles (1982) values. The counts in each bin were corrected for background values and errors estimated

**Table 1.** The clusters of galaxies in the ‘Shapley Supercluster’ with measured/estimated X-ray luminosities.

1	2		3	4	5	6	7	8	9	10	11		
Cluster	Position (1950)		$\langle v_r \rangle$	$\sigma$	Source	$N_{\text{gal}}$	$m_*$	$L_x$	$\dot{M}$	Other			
	RA	Dec	km s <sup>-1</sup>					10 <sup>44</sup> erg s <sup>-1</sup>	$M_{\odot} \text{yr}^{-1}$	Names			
A 1631	12 <sup>h</sup>	50.2 <sup>m</sup>	−15°	10′	13958	711	DS	83	15.98 ± 0.08	0.43	✓		
A 3528a	12	51.6	−28	45	16050	740	MM	72	16.37 ± 0.11	2.9	✓	K 21	
A 3528b										3.5	✓		
A 1644a	12	54.6	−17	6	14202	991	DS	92	16.50 ± 0.10	1.7	2.4	20	
A 1644b										0.68	✓		
A 3530	12	52.9	−30	5	16320		VCSZ	68	16.77 ± 0.10	0.37	✓		
A 3532	12	54.6	−30	6	16160	742	VCSZ	67	16.59 ± 0.07	1.1	1.9	✓	K 22
A 1736a	13	24.1	−26	52	13815	984	DS	104	16.13 ± 0.07	1.8	1.6	×	IC 4255
A 1736b					10412	381	DS						
A 3558	13	25.1	−31	14	14300	1250	MM	147	16.17 ± 0.08		> 4.2†		Shapley 8
SC 1329–314	13	28.6	−31	34	13300	1050	MM	105	16.28 ± 0.08	0.77			
A 3562	13	30.7	−31	25	15060	921	MM	73	16.40 ± 0.05	> 2.9	3.7	45	
A 3571	13	44.6	−32	37	11730	1060	QdS	83	16.22 ± 0.06		7.7	60	

(1) Abell number from Abell, Corwin & Olowin (1989, ACO).

(2) Position of centre from ACO. The position of the non-Abell cluster from Melnick & Moles (1987, MM).

(3, 4) Mean redshift and velocity dispersion from source (5).

(5) Sources: MM (Melnick & Moles 1987), DS (Dressler & Shectman 1988a), QdS (Quintana & da Souza, private communication), VCSZ (Vettolani *et al.* 1990, cluster with > 3 redshifts and Christiani *et al.* 1987).

(6) Number of galaxies brighter than  $B_j = 17.5$  found within  $2 h_{50}^{-1}$  Mpc (corresponding to 23 arcmin for a cluster at 15 000 km s<sup>-1</sup>) from the centre.

(7) Value of the Schechter function parameter  $m_*$ , as described in Section 3.

(8) Estimated 2–10-keV luminosity from the IPC image (see text).

(9) Measured 2–10-keV luminosity from the MPC or EXOSAT ME.

(10) Mass deposition rate from cooling flow. The ✓ symbol indicates that the presence of a flow is likely, although the image is too poor for measurement.

†Estimated from offset EXOSAT ME.

**A1631:** Dressler & Shectman (1988a, DS) find two superposed groups, one at about 5000 km s<sup>-1</sup> and a much larger one at 14 000 km s<sup>-1</sup>. The value quoted in Table 1 is an average over galaxies in the range 12 000–16 000 km s<sup>-1</sup> ( $N = 71$ ). Only the more distant one appears in the X-ray image (Fig. 3a).

**A1644:** DS find two nearby peaks at 13 000 and 14 500 km s<sup>-1</sup>. The value quoted in Table 1 is an average over galaxies in the range 12 000–16 000 km s<sup>-1</sup> ( $N = 92$ ). The X-ray image (Fig. 3b) shows a second peak around the large galaxy to the north-east.

**A1736:** DS find two superposed rich clusters (a and b), at 10 400 ( $N = 34$ ,  $9000 < v < 11 500$  km s<sup>-1</sup>), and 13 800 km s<sup>-1</sup> ( $N = 63$ ,  $11 500 < v < 16 000$  km s<sup>-1</sup>), respectively, the further one being the richer. Only this more distant one appears in the X-ray image (Fig. 3c).

**A3528:** Abell, Corwin & Olowin (1989, ACO) note the presence of a superposed poorer cluster sf. This appears as an equally X-ray luminous second cluster (Fig. 3d). Note that the two clusters are close to the edge of the IPC field of view and are constrained by the supporting ribs of the detector window.

**A3530/3532:** two nearby clusters at roughly the same distance. Abell radii overlap. A3532 is actually Klemola 22, though the other is often referred to as K22 in the literature. The X-ray image (Fig. 3e) clearly shows both clusters.

**A3562:** ‘some subclustering. Nearby cluster superposed’ (ACO). Melnick & Moles (1987, MM) find two overlapping clusters at 10 780 ( $N = ?$ ) and 15 060 km s<sup>-1</sup> ( $N = 12$ ), respectively. The other peak in the X-ray and isopleth maps corresponds to the cluster SC1329–314 listed in MM (redshift 13 300 km s<sup>-1</sup>,  $N = 10$ ), though it cannot be found in even the ACO catalogue of poorer clusters. In the X-ray image (Fig. 3f), note that Shapley 8 (A3558) is out of the IPC field of view to the west, only a small patch of emission is seen there. A3562 is bisected by one of the IPC ribs.

**A3571:** ACO note ‘slight subclustering, morphologically diverse’. The EXOSAT LE image (Fig. 3g) is less deep than the IPC images. It shows a clear peak on the central cD galaxy where the cooling flow is taking place.

from  $\sqrt{N}$ . An integral luminosity function of Schechter (1976) form was assumed,

$$\Phi(\geq m) = \phi_0 \int_t^{\infty} t^{-1} \exp(-t) dt,$$

where  $\Phi(\geq m)$  is the number of galaxies with apparent magnitude fainter than  $m$  and  $\log t = 0.4(m_* - m)$ . Values of

$m_*$  found by chi-square minimization are given in Table 1, together with  $1\sigma$  errors.

On the assumption that all clusters have the same intrinsic luminosity function  $\Phi(M)$ , where  $M$  is absolute magnitude, the value of  $m_*$  should be useful as a distance indicator (see Gudehus 1989). If the clusters in the Shapley Supercluster are expanding with the Hubble flow, then  $0.2 m_*$  should be directly proportional to  $\log v$ , where  $v$  is the cluster velocity.

If they are bound, then we can expect a strong departure from a linear relation. This is observed in Fig. 4, where, using a chi-square test, we find that the probability of agreement with the best-fitting straight line of unit slope is negligible.

The X-ray-luminosity function (Fig. 5) has been estimated by assuming a radius of  $60 h_{50}^{-1}$  Mpc for the supercluster. This corresponds to a sphere with a diameter of  $24^\circ$ , the distance between A3571 and A1631. The luminosity function is reasonably secure above a luminosity of about  $1.5 \times 10^{44}$  erg  $s^{-1}$ , corresponding to the faintest cluster (A1736) in the all-sky, flux-limited sample of Edge *et al.* (1990). The completeness of the sample is argued, in that work, to be high. The luminosity function undoubtedly *underestimates* the density of clusters of luminosity below  $\sim 1 \times 10^{44}$  erg  $s^{-1}$  where most of the additional clusters in the supercluster which were not imaged by us in X-rays must lie. The luminosity function derived from the X-ray flux-limited sample of clusters at high galactic latitude (Edge *et al.* 1990) is plotted for comparison. It shows, as expected, that there is a strong overdensity of clusters in the supercluster, by a factor of between 10 and 25, and that the supercluster contains a higher proportion of high-X-ray-luminosity clusters. The region clearly is not spherical in shape and has a smaller volume than that of the circumscribed sphere. A simple reduction can be made by assuming that the northern extensions (A1631 and A1644) are part of a subsupercluster and that the core region with its eastern extension is spherical and of radius  $37 h_{50}^{-1}$  Mpc. The overdensity of clusters relative to the field is then twice the above estimates, i.e. a factor of between 20 and 50.

The X-ray luminosity function shows that the merger rate in the Shapley Supercluster is between 1.5 and 3 times higher

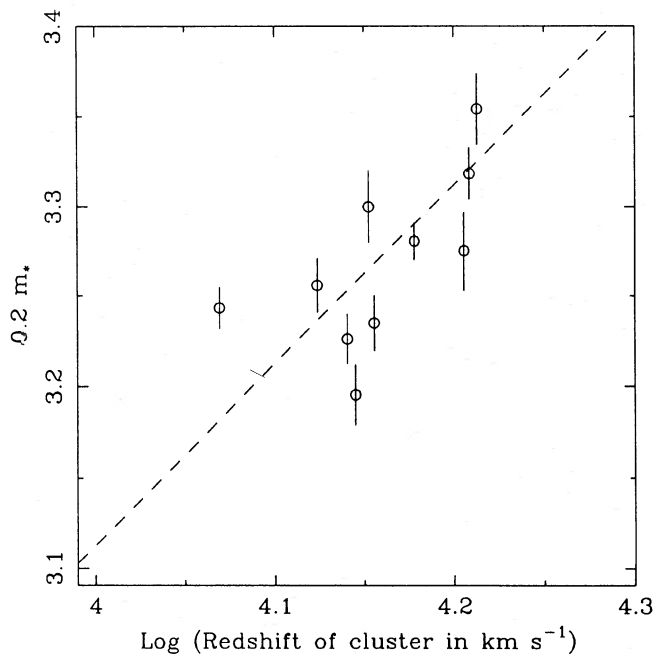


**Figure 4.** The characteristic Schechter (1976) magnitude  $m_*$ , divided by five so that the axes are of equal scale, plotted against log (redshift) for a few clusters. The clusters belonging to the 'Shapley Supercluster' show an opposite trend to that expected from a uniform Hubble flow (represented by the dashed line, which is the best-fitting straight line of slope unity).

than elsewhere, if we interpret its shape using the subcluster-merging model for the evolution of clusters given by Edge *et al.* (1990). This suggests that the velocities of the subclusters are higher, presumably due to the deeper gravitational well. In merging to produce the present cluster, the subclusters collide at several thousand  $\text{km s}^{-1}$  [e.g. the simulations by McGlynn & Fabian (1984) in which the clusters pass through each other before finally merging]. Some gas may be shocked to temperatures exceeding that for escape from the cluster and so create an 'intrasupercluster medium'. The Shapley Supercluster is a good candidate for a search for such gas.

## 5 MASS ESTIMATES

If the Shapley Supercluster is a bound entity, then it is the most massive known. By 'bound', we mean that it has separated from the overall expansion of the Universe, and its own self-gravity is retarding the cosmic expansion at its edges, turning most of the expansion round into a collapse for most of the observed region. The distribution of  $m_*$  (Fig. 4) shows that there are large departures from the Hubble flow in the Shapley Supercluster, which supports the hypothesis that it is bound. The time taken by clusters moving at  $\sim 3000$   $\text{km s}^{-1}$  to cross 30 Mpc is  $\sim 10^{10}$  yr, so some large-scale interaction can have taken place.

First, we estimate an upper bound to the mass of the supercluster by assuming that the virial theorem can be applied,

$$GM = 7.5 R_h \sigma^2$$

(Binney & Tremaine 1987). This estimate is uncertain since the supercluster is most unlikely to be virialized. However, if much of the observed spread of velocities is gravitational in origin, then an expression similar to the one above must

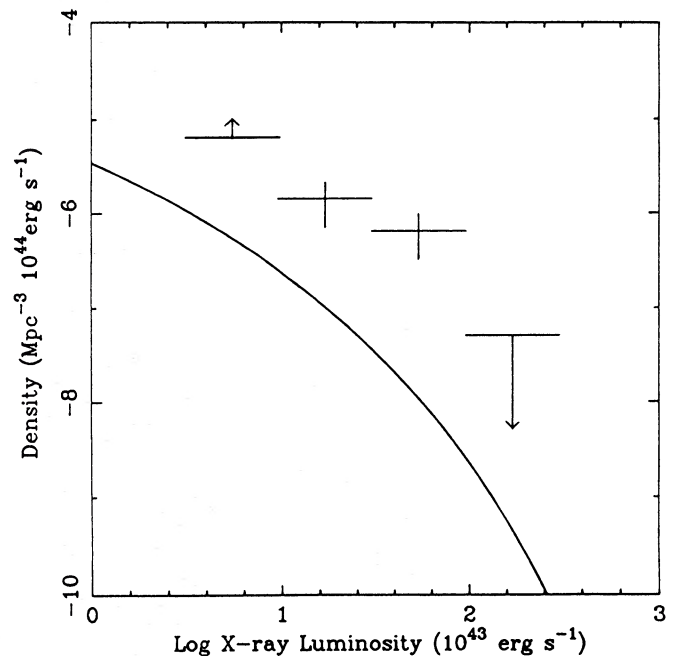


**Figure 5.** The X-ray-luminosity function of the Shapley Supercluster compared with the luminosity function found from the 46 X-ray-brightest clusters (solid curve) from Edge *et al.* (1990).

apply.  $R_h$  is the half-mass radius and  $\sigma$  is the line-of-sight velocity dispersion which we estimate as  $40 h_{50}^{-1}$  Mpc and  $1800 \text{ km s}^{-1}$  from the standard deviations of the distributions of the 12 X-ray-cluster positions and velocities. (The velocity dispersion is  $\sim 1580 \text{ km s}^{-1}$  if we include other clusters in the supercluster not observed in X-rays.) This gives, for the Shapley Supercluster,

$$M_{SS} \approx 2 \times 10^{17} h_{50}^{-1} M_{\odot}.$$

A very similar mass is obtained by scaling to the Coma cluster,

$$M = M_{\text{Coma}} \left( \frac{\sigma}{\sigma_{\text{Coma}}} \right)^2 \left( \frac{R}{R_{\text{Coma}}} \right),$$

where  $\sigma$  is the relevant velocity dispersion and  $R$  is the radius. We use  $1050 \text{ km s}^{-1}$ ,  $1 h_{50}^{-1}$  Mpc for the Coma cluster (this radius agrees with the first virial formula) and assume the mass of the Coma cluster to be  $1.9 \times 10^{15} h_{50}^{-1} M_{\odot}$  (Hughes 1989). The mass is reduced to  $7 \times 10^{16} h_{50}^{-1} M_{\odot}$  if we exclude the northern extension of A1631 and A1644. Our estimates are upper limits if most of the velocity spread across the supercluster is due to the Hubble flow. As already discussed, Fig. 4 provides marginal evidence against this.

Secondly, we estimate the mass of the supercluster by summing the masses of the individual clusters. This is a reliable minimum estimate. The individual cluster masses have been obtained by scaling to the Coma cluster,  $L_x(2\text{--}10 \text{ keV}) = 8 \times 10^{44} h_{50}^{-2} \text{ erg s}^{-1}$ , assuming  $L_x \propto M^{0.4}$  (Edge & Stewart 1990). The X-ray images are particularly important here in showing that we are dealing with deep potential wells; the available spectral data of the clusters observed in the 2–10-keV band show that they are typical for their luminosities. We obtain a total mass for the 12 clusters of at least  $6.8 \times M_{\text{Coma}}$ , or

$$M_{SS} > 1.4 \times 10^{16} h_{50}^{-1} M_{\odot}.$$

The optical-luminosity functions for these 12 clusters integrate to give a total light for the clusters of  $3.6 \times 10^{13} h_{50}^{-2} L_{B\odot}$  and the resulting mass-to-light ratio of  $400 h_{50}$  is large but not unreasonable for rich clusters (note that our value corresponds to  $M/L_{\text{bol}} \sim 140 h_{50}$ ). Repeating the estimate for the core region gives a mass of  $1.1 \times 10^{16} h_{50} M_{\odot}$  and mass-to-light ratio of  $350 h_{50}$ .

The mass-to-light ratio obtained from the virial mass estimate is uncertain, since we only have a rough estimate of the light associated with galaxies outside a projected  $2 h_{50}^{-1}$  Mpc radius of the cluster centres owing to a lack of redshift measurements for the identification of supercluster galaxies. The light is probably not more than twice that associated with the clusters (from the total number of galaxies seen), so the mass-to-light ratio of the system, if it is bound and the velocity spread of the clusters is wholly dynamical, is about  $\geq 2000 h_{50}$ . This value is high, several times that found for rich clusters. The masses of rich clusters are obtained from their central few Mpc and could be higher if they are surrounded by an extensive halo of dark matter. Alternatively, the application of the virial theorem may be flawed, in principle because the region is not virialized, or in practice because of small number statistics or projection effects.

The masses estimated above apply to regions of radius  $60 \Omega_0 h_{50}^{-1}$  and  $37 h_{50}^{-1}$  Mpc, respectively. The masses expected within such regions in a homogeneous universe are  $6 \times 10^{16} \Omega_0 h_{50}^{-1}$  and  $1.4 \times 10^{16} \Omega_0 h_{50}^{-1} M_{\odot}$ , where  $\Omega_0$  is the density parameter of the universe. They mean that the ratio of the average density associated with the supercluster to the mean cosmic density is

$$\frac{\rho}{\bar{\rho}} \approx 1.6, 5, 0.23 \text{ and } 0.8 \Omega_0^{-1}$$

(the value of  $\rho/\bar{\rho}$  is independent of the value of the Hubble constant used) for the virial masses for the whole and core regions, and the luminosity-scaled masses for the whole and core regions, respectively. It is clear that  $\rho/\bar{\rho} \geq 1 \Omega_0^{-1}$  in the core region of diameter  $74 h_{50}^{-1}$  Mpc in terms of *mass associated with X-ray-detected clusters*. Other galaxies in the region which are not members of the clusters reported here will increase these estimates.

If  $\Omega_0$  is considerably less than unity, our estimates for  $\rho/\bar{\rho}$  represent large overdensities over a large volume. If  $\Omega_0 \approx 1$ , we cannot say whether there is an overdensity in the case of the luminosity-scaled masses without some knowledge of the nature of the dark matter and whether it might just be distributed with the clusters in this particular region.

## 6 DISCUSSION

We have shown that the remarkable ‘cloud of galaxies’ in Centaurus discovered by Shapley is also notable in X-rays. The X-ray data have enabled us to overcome projection effects in such a populated region and identify the individual clusters. Many of the component clusters are seen to be double and possibly multiple clusters. Each of these clusters and subclusters is more X-ray luminous than the Virgo cluster (and the Local Supercluster).

We have estimated the mass of the Shapley Supercluster as between  $1.4 \times 10^{16}$  and  $\sim 2 \times 10^{17} M_{\odot}$  within a sphere of diameter 120 Mpc and  $1.1 \times 10^{16}$  to  $7 \times 10^{16} M_{\odot}$  in the ‘core’ region of diameter 74 Mpc ( $H_0 = 50 \text{ km s}^{-1} \text{ Mpc}^{-1}$ ). The lower estimate, which is a strong limit, gives a value of  $\rho/\bar{\rho} \approx 1 \Omega_0^{-1}$  in the core region. This is an exceptionally large mass. Our result emphasizes that there is considerable power on large scales in the mass distribution of the Universe.

The only comparable (or larger) mass is that of the Great Attractor, which lies in front of the supercluster. It is curious that there are so few clusters in the Great Attractor, with only the Centaurus cluster being as X-ray luminous (and presumably as massive) as any observed here (it is comparable with the eleventh most luminous one in Table 1). The mass of the Great Attractor is estimated from the peculiar velocities of galaxies in the surrounding region and requires that it has a very high mass-to-light ratio. The high mass in the Shapley Supercluster is accountable in terms of clusters similar to well-measured objects such as the Coma cluster. The way in which mass is converted into X-ray-luminous matter must have been quite different in the Shapley Supercluster from that in the Great Attractor region. The ‘bias factor’ of cluster formation may therefore be spatially variable.

An interesting question for the origin of large-scale structure in the Universe is whether the initial spectrum of matter perturbations had a Gaussian distribution. Kaiser &

Davis (1985) have previously considered this problem in connection with the Corona Supercluster (a supercluster with only one X-ray-bright cluster compared with six in the Shapley Supercluster). Their method consists of comparing the (linear) fluctuations associated with a supercluster with that expected from the galaxy correlation function on the scale of the supercluster. We assume for the Shapley Supercluster that  $\rho/\bar{\rho} > 0.8 \Omega_0^{-1}$  on a scale (radius) of  $37 h_{50}^{-1}$  Mpc and use  $\sigma(R) = (R/16 h_{50}^{-1} \text{ Mpc})^{-1} b^{-1}$  (from Kaiser & Davis 1985) for the rms fluctuation on scale  $R$ . The bias factor  $b$  is defined such that fluctuations in mass are amplified  $b$  times in galaxy density ( $b \sim 2$ , Kaiser & Lahav 1989). The significance of our supercluster depends on  $\Omega_0$ . If  $\Omega_0 = 0.2$  then  $\rho/\bar{\rho} > 4$  and the corresponding linear density perturbation is  $\Delta_L \sim 1$  on a scale of  $(\rho/\bar{\rho})^{1/3} \times 37 = 59 h_{50}^{-1}$  Mpc. Consequently, the Shapley Supercluster is a fluctuation exceeding  $3.2 b\sigma$ . On the other hand, if  $\Omega_0 = 1$  the situation is unclear. Either the bias is very unusual in this region and all the dark matter has clumped into clusters ( $\rho/\bar{\rho} = 0.8$ ), or the universal dark matter is uniform there and the clusters are an additional mass. Then  $\rho/\bar{\rho} \geq 2$  and the fluctuation is  $\geq 1.3 b\sigma$  on a scale of  $43 h_{50}^{-1}$  Mpc. These estimates of the significance of the supercluster are increased by a factor of between 1.6 and 1.9 if we assume that the galaxy-galaxy correlation function does not extend further than  $16 h_{50}^{-1}$  Mpc.

In X-ray terms, the Shapley Supercluster is the only such object within  $z < 0.1$ , the depth at which the two X-ray-brightest clusters would just reach the end of the Edge *et al.* (1990) list of X-ray-brightest clusters (flux limit of  $1.7 \times 10^{-11}$  erg cm $^{-2}$  s $^{-1}$  for  $|b| > 20^\circ$ ). Consequently, we might expect to see a  $3\sigma$  fluctuation (from the probability distribution used by Kaiser & Davis), but not a significantly larger one if the fluctuations are Gaussian. We conclude that the Shapley Supercluster has an exceptional overdensity unless  $\Omega_0 \sim 1$ ,  $b \lesssim 2$ , the galaxy-galaxy correlation function extends to scales  $\sim 45 h_{50}^{-1}$  Mpc and there is no more mass in the supercluster than that directly associated with the X-ray-bright clusters (the peculiar motions of the member clusters evident in Fig. 4 cannot then be due to the mass of the supercluster).

A deep gravitational potential well such as the Shapley Supercluster would produce, at the epoch of recombination, a deviation in the temperature of the microwave background by the Sachs-Wolfe effect (1967). The Sachs-Wolfe deviation is

$$\frac{\Delta T}{T} = \frac{1}{3} \phi c^{-2}$$

or  $2.8 \times 10^{-5}$  for the virial mass in  $60 h_{50}^{-1}$  Mpc, or  $> 4 \times 10^{-6}$  for the total X-ray-luminosity-scaled cluster mass. The effect should be detectable over a scale exceeding  $0.5$  and is comparable with current upper limits. If the mass of the Shapley Supercluster is  $\sim 5 \times 10^{16} h_{50}^{-1} M_\odot$  (the median of our estimates) then it imparts to us a peculiar velocity of about  $50 \text{ km s}^{-1}$ , or about 10 per cent of our motion with respect to the microwave background. This agrees with the independent estimate of Raychaudhury (1989), who found the contribution of the Shapley Supercluster to the optical dipole to be 10–15 per cent.

The optical-luminosity functions suggest that there are large deviations from the Hubble flow within the super-

cluster, indicating that it may be bound. The X-ray-luminosity function shows that the region has a cluster overdensity of between 10 and 50, the uncertainty arising from the volume assumed for the region. Such a large overdensity is consistent with the region being bound, especially in the core region around Shapley 8.

Observationally, our study of the Shapley Supercluster has demonstrated that the region is exceptional in its density of rich clusters and the multiple nature of the clusters. We cannot say conclusively whether the supercluster is one bound entity, or two (the core and the northern extension), or more. The statistics of the number of bright X-ray clusters show that we are not dealing with a chance aggregation of clusters. Provided that the component clusters are not on non-interacting circular orbits within the supercluster and that their core radii do not change, the region should continue to evolve rapidly and, in another ten billion years or so, will generate some of the most X-ray-luminous clusters in the Universe, with quasar-like luminosities.

## ACKNOWLEDGMENTS

We thank D. Lynden-Bell and D. Weinberg for help and discussions, and M. Irwin and the APM group in Cambridge for scanning the UKST plates involved in this work. ACF and ACE thank the Royal Society and SR thanks the SERC and St. Edmund's College for support.

## REFERENCES

- Abell, G. O., Corwin, H. G. & Olowin, R. P., 1989. *Astrophys. J. Suppl.*, **70**, 1 (ACO).
- Allen, D. A., Norris, R. P., Staveley-Smith, L., Meadows, V. S. & Roche, P. F., 1990. *Nature*, **343**, 45.
- Arnaud, K. A., 1988. In: *Cooling Flows in Clusters and Galaxies*, p. 31, ed. Fabian, A. C., Kluwer, Dordrecht.
- Binney, J. & Tremaine, S., 1987. *Galactic Dynamics*, Princeton University Press, Princeton.
- Burstein, D. & Heiles, C., 1982. *Astr. J.*, **87**, 1165.
- Cristiani, S., de Souza, R., D'Odorico, D., Lund, G. & Quintana, H., 1987. *Astr. Astrophys.*, **179**, 108.
- Dressler, A. & Shectman, S. A., 1988a. *Astr. J.*, **95**, 284.
- Dressler, A. & Shectman, S. A., 1988b. *Astr. J.*, **95**, 985.
- Edge, A. C., 1989. *Ph.D. thesis*, University of Leicester.
- Edge, A. C. & Stewart, G. C., 1990. In preparation.
- Edge, A. C., Stewart, G. C., Fabian, A. C. & Arnaud, K. A., 1990. *Mon. Not. R. astr. Soc.*, **245**, 559.
- Forman, W., Bechtold, J., Blair, W., Giacconi, R., Van Speybroeck, L. & Jones, C., 1981. *Astrophys. J.*, **243**, L133.
- Gudehus, D. H., 1989. *Astrophys. J.*, **342**, 617.
- Hughes, J. P., 1989. *Astrophys. J.*, **337**, 21.
- Jahoda, K. & Mushotzky, R. M., 1989. *Astrophys. J.*, **336**, 638.
- Kaiser, N. & Davis, M., 1985. *Astrophys. J.*, **297**, 365.
- Kaiser, N. & Lahav, O., 1989. *Mon. Not. R. astr. Soc.*, **237**, 129.
- Kibblewhite, E. J., Bridgeland, M. T., Bunclark, P. & Irwin, M. J., 1984. In: *Astronomical Microdensitometry Conference*, p. 277, ed. Klinglesmith, D. A., NASA CP-2317.
- Kriss, G. A., Cioffi, D. F. & Canizares, C., 1983. *Astrophys. J.*, **272**, 439.
- Lahav, O., Edge, A. C., Fabian, A. C. & Putney, A., 1989. *Mon. Not. R. astr. Soc.*, **238**, 881.
- Lynden-Bell, D., Faber, S. M., Burstein, D., Davies, R. L., Dressler, A., Terlevich, R. J. & Wegner, G., 1988. *Astrophys. J.*, **326**, 19.
- McGlynn, T. A. & Fabian, A. C., 1984. *Mon. Not. R. astr. Soc.*, **208**, 709.

- Maddox, S. J., Efstathiou, G. & Sutherland, W. J., 1990. *Mon. Not. R. astr. Soc.*, **246**, 433.
- Melnick, J. & Moles, M., 1987. *Rev. Mex. Astr. Astrofis.*, **14**, 72.
- Pesce, J. E., Fabian, A. C., Edge, A. C. & Johnstone, R. M., 1990. *Mon. Not. R. astr. Soc.*, **244**, 58.
- Raychaudhury, S., 1989. *Nature*, **342**, 251.
- Raychaudhury, S., 1990. *Ph.D thesis*, University of Cambridge.
- Sachs, R. K. & Wolfe, A. M., 1967. *Astrophys. J.*, **147**, 73.
- Scaramella, R., Baiesi-Pillastrini, G., Chincarini, G., Vettolani, G. & Zamorani, G., 1989. *Nature*, **338**, 562.
- Schechter, P., 1976. *Astrophys. J.*, **203**, 297.
- Schwartz, D. A., Schwarz, J. & Tucker, W. A., 1980. *Astrophys. J.*, **238**, L59.
- Shapley, H., 1930. *Bull. Harvard Obs.*, **874**, 9.
- Vettolani, G., Chincarini, G., Scaramella, R. & Zamorani, G., 1990. *Astr. J.*, **99**, 1709.